EAST EUROPEAN JOURNAL OF PHYSICS. 1. 233-240 (2026)
DOI:10.26565/2312-4334-2026-1-25 ISSN 2312-4334

FEATURES OF THE THERMAL BEHAVIOR AND PHASE FORMATION OF $BiFeO_3$ USING PRECURSORS ACTIVATED BY SOLAR MELTING

M.S. Payzullakhanov[1,2], F.A. Giyasova[3], M.A. Yuldoshev[4]*, Ch.X. Toshpulatov[5], R.U. Ernazarov[5], F.A. Giyasov[3], A. Urishev[6], A.D. Paluanova[7]

[1]Institute of Materials Science, Academy of Sciences of the Republic of Uzbekistan. Tashkent, Uzbekistan
[2]Fergana State Technical University, Uzbekistan
[3]Kimyo International University in Tashkent, Uzbekistan
[4]Turan International University, Namangan, Uzbekistan
[5]Tashkent branch of Samarkand State University of Veterinary Medicine, Animal Husbandry and Biotechnology, Uzbekistan
[6]Tashkent Institute of Irrigation and Agricultural Mechanization Engineers, National Research University, Uzbekistan
[7]Nukus State Pedagogical Institute, Uzbekistan
**Corresponding Author e-mail: murod.yuldoshev1993@gmail.com*
Received December 1, 2025; revised January 16, 2026; accepted January 30, 2026

The effect of pretreatment of Bi_2O_3 and Fe_2O_3 oxides on the synthesis and structural characteristics of bismuth ferrite $BiFeO_3$ was studied. It was found that $BiFeO_3$ formation begins at 790÷850 °C, and decomposition occurs above ~920 °C. Preliminary melting of the oxides in a solar furnace shifts the thermal effects to higher temperatures and increases the thermodynamic stability of the phase. X-ray phase analysis revealed the formation of a perovskite-like structure with orthorhombic distortion, high crystallinity, and a crystallite size of 40±10 nm. Phase analysis confirmed an increase in the content of the main phase to 97 % and a decrease in the impurity phase $Bi_2Fe_4O_9$. The obtained results confirm the efficiency of preliminary solar melting of oxides for the synthesis of high-quality ceramic materials based on $BiFeO_3$.
Keywords: *Solar furnace; Synthesis; Bismuth ferrite; Phase; Diffusion; Microstructure; Analysis; Temperature; Thermal effect*
PACS: 68.37.Hk, 78.70.Ck, 77.84.-s

INTRODUCTION

Multiferroic materials, which combine spontaneous polarization and magnetic ordering in a single structure, are of significant interest for modern electronics, spintronics, and sensor technologies [1-3]. Among these compounds, bismuth ferrite $BiFeO_3$ (BFO), which exhibits ferroelectric and antiferromagnetic properties at room temperature, has attracted particular attention. Due to its high Néel temperature (≈370 °C) and Curie point (≈820 °C), $BiFeO_3$ is considered a promising material for the creation of energy-efficient multifunctional devices, piezoelectric transducers, and photocatalytic systems [4-6].

Despite its high functional characteristics, obtaining single-phase bismuth ferrite $BiFeO_3$ remains a complex task. With traditional synthesis methods, secondary phases such as $Bi_2Fe_4O_9$ and $Bi_{25}FeO_{39}$ are typically formed from an oxide mixture of Bi_2O_3 and Fe_2O_3, thereby reducing the material's electrical and magnetic properties [7-10]. Attempts to eliminate their formation by changing the stoichiometry of the initial components, by introducing excess Bi_2O_3, also do not result in obtaining a single-phase compound [11]. The phase composition and morphology of the samples are significantly affected by the composition and dispersion of the precursors, the degree of their homogenization, and the heat treatment conditions [12]. As noted in [13], the difficulties in synthesizing single-phase bismuth ferrite are due to the peculiarities of the phase diagram of the Bi_2O_3-Fe_2O_3 system, which includes several stable compounds, as well as the high volatility of Bi_2O_3 at temperatures above the melting point [14] and the thermodynamic instability of $BiFeO_3$ in air in the absence of an equilibrium melt [15]. A comparison of literature data [13,16,17] indicates that obtaining single-phase $BiFeO_3$ by solid-phase synthesis is practically impossible.

In recent years, considerable attention has been paid to solution combustion synthesis (SCS) methods based on the exothermic reaction between metal nitrates and organic fuels (glycine, urea, citric acid, etc.) [18,19]. These methods allow the production of nanodispersed powders in a short time at temperatures of 500÷600 °C. However, the unevenness of the thermal field and the rapid evolution of gases lead to the formation of a porous structure and secondary phases, as well as to contamination of the product with carbon residues [20,21].

An alternative approach to synthesizing oxide materials is the use of concentrated solar radiation (CSR). The use of a solar furnace provides local heating up to 2000÷2500 °C and a heating rate up to 200 °C/s, enabling melting and crystallization without external fuel [22, 23]. In [24], it was shown that melting the oxide precursors Bi_2O_3 and Fe_2O_3 at the focus of a solar furnace leads to the formation of dense, homogeneous $BiFeO_3$ structures with a low coefficient of thermal expansion and high chemical resistance. Solar synthesis is environmentally friendly, highly energy-efficient, and allows the production of materials with minimal secondary-phase content [25].

Cite as: M.S. Payzullakhanov, F.A. Giyasova, M.A. Yuldoshev, Ch.X. Toshpulatov, R.U. Ernazarov, F.A. Giyasov, A. Urishev, A.D. Paluanova, East Eur. J. Phys. 1, 233 (2026), https://doi.org/10.26565/2312-4334-2026-1-25

As a result of the above, traditional methods for synthesizing bismuth ferrite – both thermal (solid-phase reactions at temperatures below the melting point) and chemical (solution reactions) – fail to produce single-phase $BiFeO_3$. Therefore, the use of solar technologies based on exposure to concentrated, high-density light is of scientific interest. In this approach, synthesis is performed from a melt formed under the influence of concentrated solar radiation, where phase formation occurs directly in the melt, and the resulting state is fixed by quenching.

Combining fuel precursors with high-energy solar heating opens the prospect of creating next-generation multiferroic materials. This approach combines the chemical homogeneity of the precursors with the high thermal efficiency of a solar furnace, facilitating the formation of dense single-phase structures with improved physical, mechanical, and functional properties. This study examines the influence of concentrated solar radiation parameters and the composition of fuel precursors on the structure formation, phase composition, and properties of bismuth ferrite ($BiFeO_3$).

The aim of this study is to determine the effect of pre-melting Bi_2O_3 and Fe_2O_3 oxides in a solar furnace on the structure formation, phase composition, and properties of $BiFeO_3$, and to compare the results with traditional solid-phase synthesis to optimize the conditions for producing a single-phase material.

EXPERIMENTAL SAMPLES AND MEASUREMENT METHODS

To determine the influence of the microstructural state of the components (Bi_2O_3 and Fe_2O_3 oxides) on the synthesis process and properties of bismuth ferrite, the starting components were melted in a small-sized solar installation — a small solar furnace (SSF) with a high degree of concentration [26]. The technological route included the following operations: grinding of the starting components → mixing → molding → melting → quenching. The density of the concentrated flux was 450 W/cm², enabling local heating of the sample to temperatures exceeding the melting points of the components. The exposure in the molten state was 15 minutes, which contributed to the complete homogenization of the oxide mass. The resulting melts were quenched in water at a cooling rate of about 10^4 °C/s, thereby fixing the system's nonequilibrium state and preventing phase separation.

The solidified samples were ground in a ball mill under wet conditions for 10 hours at a material:water:grinding media weight ratio of 1:1:1. After grinding, the powder was sieved through a 0.05 mm sieve to ensure a uniform particle size distribution. A Bi_2O_3+Fe_2O_3 mixture was prepared from the resulting fused oxides in a strictly stoichiometric ratio corresponding to the $BiFeO_3$ composition. The prepared powder was pressed into tablets under a 1-ton load on a C-100 hydraulic press. The resulting pressed samples were heat-treated in a resistance electric furnace with silicate heaters at various temperatures. These samples were designated as type A.

For comparative analysis, bismuth ferrite was also synthesized without the solar melting step, directly from the starting mixture of Bi_2O_3 and Fe_2O_3 oxides. The resulting samples, which underwent standard heat treatment, were designated type B and used as controls.

In this study, modern physicochemical methods were used to analyze the pyroxene materials, ensuring high accuracy and minimal error in the comprehensive assessment of their properties. The phase and thermal characteristics of oxide systems and man-made rock waste were investigated using differential thermal analysis (DTA) and thermogravimetric analysis (TGA). Experiments were conducted on a Q-1500 D derivatograph in the temperature range of 100÷1000 °C at a heating rate of 15°C/min. This allowed for simultaneous recording of mass changes and thermal effects, as well as identification of the nature of phase transformations, dehydration processes, and thermal decomposition of the studied samples.

To identify the phase composition, X-ray diffraction (XRD) was performed on a DRON-3M diffractometer with a copper anode (CuKα radiation).

The physical characteristics of the samples were assessed using density parameters. The apparent density (ρ_{app}) was determined by hydrostatic weighing in octane, and the X-ray density (ρ_x) was calculated using the expression [27]:

$$\rho_x = 1.66 \times M / V, \quad (1)$$

where, M is the mass of the formula unit (g), V is the volume of the unit cell of the perovskite structure (Å^3).

Relative density (ρ_{rel}) was calculated as the ratio $\rho_{kak}/\rho_x p$, expressed as a percentage:

$$\rho_{rel} = (\rho_{app} / \rho_x) \times 100\%. \quad (2)$$

To assess the packing density of the crystal lattice, the structural looseness parameter (ω) was additionally calculated using the formula [28]:

$$\omega = M / (n\rho), \quad (3)$$

where, M is the molecular mass of the compound, n is the number of structural units (atoms, ions or complexes) in the formula cell, ρ is the density of the material.

RESULTS AND DISCUSSION

The DTA curves of a mixture of bismuth and iron oxides (Bi_2O_3 + Fe_2O_3), obtained for samples subjected and not subjected to melting in a solar furnace, in the temperature range of 100÷1000 °C, are shown in Fig. 1.

As is well known, such m-n-n^+-m structures are often used to study transient effects and rectification characteristics.

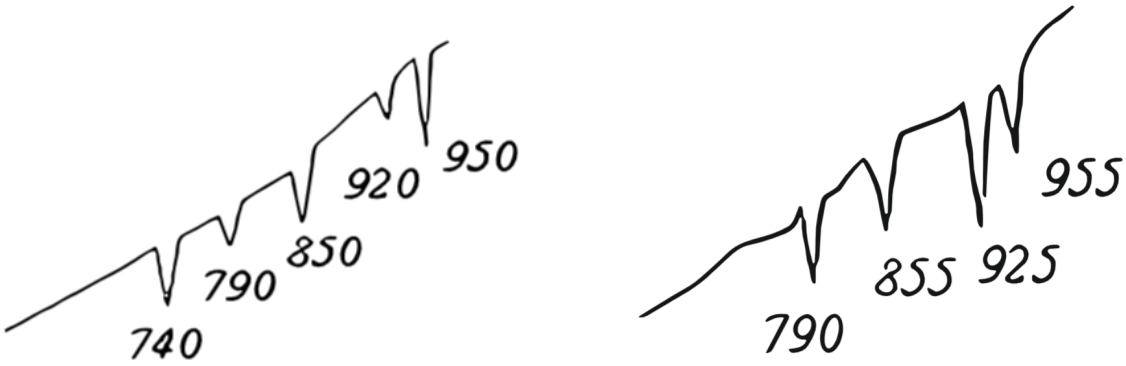

a b

Figure 1. DTA of a Bi_2O_3 + Fe_2O_3 mixture in the temperature range of100÷1000°C
a) components not subjected to melting in a solar furnace; b) components melted in a solar furnace

From Fig. 1a, it follows that in the first case five endothermic peaks are recorded on the DTA curve, the nature of the dependence indicating the sequential occurrence of a number of endothermic processes as the temperature increases. The endothermic effect observed at a temperature of about 740 °C corresponds to the polymorphic transformation of bismuth oxide (Bi_2O_3) – the transition of the low-temperature β-modification to the high-temperature δ-form, which is consistent with the literature data [4, 29] on the behavior of this compound upon heating. At ~790 °C, an endothermic peak is observed, associated with the melting of the eutectic mixture in the Bi_2O_3-Fe_2O_3 system and the onset of interaction of oxides with the formation of primary $BiFeO_3$ crystals. A further increase in temperature to ~850 °C is accompanied by intense formation of the $BiFeO_3$ phase due to the activation of diffusion processes between the melt components. At temperatures of 920÷950 °C, endothermic effects are observed, indicating the decomposition of bismuth ferrite with the formation of secondary phases, mainly $Bi_2Fe_4O_9$ and $Bi_{25}FeO_{39}$. The results of thermal analysis show that the synthesis of bismuth ferrite ($BiFeO_3$) from the initial mixture of Bi_2O_3 and Fe_2O_3 oxides begins in the range of 790÷850 °C, while the thermal stability of the resulting compound is maintained up to approximately 920 °C, after which its partial decomposition begins [30].

A comparison of the obtained thermograms (Fig. 1 a and b), reveals the influence of preliminary melting of the oxide precursors on the thermal behavior of the Bi_2O_3-Fe_2O_3 system. While the mixture that has not been subjected to solar melting is characterized by a sequential occurrence of endothermic processes with pronounced decomposition of bismuth ferrite at temperatures above 900 °C, in the case of pre-melted components, a shift in the temperature effects and a decrease in their intensity are observed. This indicates a change in the mechanism of oxide interaction and an increase in the stability of the resulting $BiFeO_3$ phase [31–33].

Fig. 1b shows the DTA curve of a mixture of bismuth and iron oxides (Bi_2O_3+Fe_2O_3), pre-melted in a solar furnace, recorded in the temperature range of 100÷1000 °C. The nature of the thermogram differs significantly from the similar dependence for the initial unmelted components, which indicates a change in the physicochemical properties of the system under the influence of concentrated solar radiation. In the temperature range of about ~790 °C, a weak endothermic effect is observed, corresponding to the onset of interaction of the oxides, accompanied by activation of their surface and the nucleation of the bismuth ferrite phase $BiFeO_3$. A more intense endothermic peak at ~855 °C reflects the main stage of $BiFeO_3$ formation associated with the melting of the eutectic mixture and diffusion redistribution of the components [34,35]. The endothermic effects at 925 and 955 °C are due to the partial decomposition of $BiFeO_3$ with the formation of secondary phases $Bi_2Fe_4O_9$ and $Bi_{25}FeO_{39}$. However, the intensity of these effects is significantly lower than for unmelted samples, indicating an increase in the thermal stability of bismuth ferrite synthesized from the solar-melted mixture. The DTA results indicate that preliminary melting of the initial bismuth and iron oxides (Bi_2O_3 and Fe_2O_3) in a solar furnace promotes a more complete reaction of bismuth ferrite $BiFeO_3$ formation, as well as an increase in the stability of its phase over a wider temperature range. This is due to an increase in the chemical activity of the components after solar melting, which ensures more intense interaction between them [36]. Additionally, it was established that the endothermic effects corresponding to phase transformations shift to the region of higher temperatures by approximately 50 °C, which indicates an improvement in the thermodynamic stability of the system and the formation of a more stable $BiFeO_3$ structure.

Diffraction peaks in the range 2θ ≈ 20÷60°, characteristic of the perovskite-like structure of $BiFeO_3$, are shown in Fig. 2.

The X-ray diffraction pattern of bismuth ferrite $BiFeO_3$ synthesized at 885 °C shows phase X, corresponding to a solid solution of $Bi_2Fe_4O_9$, which is [Fe_2O_3 2$BiFeO_3$]. Bismuth ferrite was synthesized by a solid-phase reaction from the initial oxides Bi_2O_3 and Fe_2O_3. After mixing and molding, the samples were calcined at 885 °C for 2 hours. X-ray diffraction analysis was performed using CuKα radiation (λ=1.5406 Å) in the angular range 2θ=20÷60°. Interplanar distances were determined according to Bragg's law [37]:

$$d=\lambda/2\sin\theta, \quad (4)$$

The lattice parameters were calculated using the pseudocubic structure approximation:

$$a=d\,(h^2+k^2+l^2)^{1/2}, \quad (5)$$

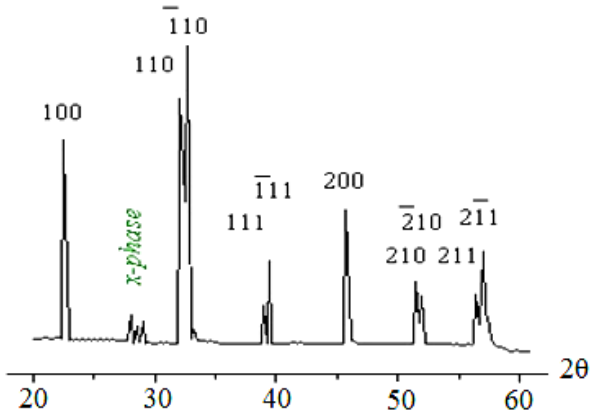

Figure 2. X-ray diffraction pattern of $BiFeO_3$ calcined at 885°C

The presence of narrow and distinct maxima indicates a high degree of crystallinity of the sample. In the range of angles 2θ=20÷60°, distinct and intense diffraction maxima are observed, corresponding to reflections from the planes (100), (110), (–110), (111), (–111), (200), (210), (–210), and (211). The set of registered reflections indicates the formation of a perovskite-like structure of bismuth ferrite with an orthorhombic distortion of the unit cell, belonging to the space group R3c. The calculated interplanar distances and lattice parameters are presented in Table 1.

Table 1. Lattice parameters of $BiFeO_3$ calcined at 885°C

Reflex (hkl)	2θ (°)	d (Å)	Pseudocubic constant a (Å)
(100)	22.6	3.931	3.931
(110)	31.6	2.829	4.001
(111)	39.8	2.263	3.920
(200)	46.5	1.964	3.928

Bismuth ferrite is characterized by an orthorhombic distortion of the perovskite cell [38] and temperature-dependent nonstoichiometry [39], which complicates the synthesis of a single-phase compound. In the studied sample, a high degree of crystallinity is achieved at a temperature of 885 °C, and a stable $BiFeO_3$ phase is formed without signs of secondary compounds. The average lattice parameter, calculated from the main diffraction peaks, is a=3.94±0.04 Å, which corresponds to the values characteristic of an orthorhombically distorted perovskite. The X-ray density of bismuth ferrite, calculated based on the structural parameters, is $\rho=8.39$ g/cm^3. The obtained data confirm the formation of phase-pure $BiFeO_3$ with a stable crystalline structure and a high degree of ordering of the atomic lattice.

The absence of additional reflections characteristic of Bi_2O_3, Fe_2O_3 oxides or $Bi_2Fe_4O_9$ phases indicates the formation of single-phase $BiFeO_3$. The presence of a weakly expressed signal, designated as the x-phase, may be associated with an insignificant content of the transition phase; however, its intensity is low and does not significantly affect the overall phase composition. The shape and width of the peaks indicate a high degree of crystallinity of the material. Narrow and symmetrical maxima reflect the growth of crystallites at the optimal synthesis temperature. The average crystallite size can be calculated using the Scherrer formula [40], where $K \approx 0.9$:

$$D = K\cdot L/\beta\cdot\cos\theta, \quad (6)$$

Experimental FWHM values (0.2±0.05°) were used to estimate the crystallite size, yielding an approximate size of D=40±10 nm.

These results indicate that at 885 °C, an optimal balance is achieved between the diffusion rate and the stability of the $BiFeO_3$ phase, ensuring the formation of a structurally ordered material without secondary phases.

The microstructure of $BiFeO_3$ heat-treated at 885 °C is shown in Fig. 3. Scanning electron microscopy (SEM) analysis indicates the formation of a fine-grained, porous structure characteristic of partially sintered perovskite materials.

As shown in Figure 3a, the type A sample exhibits a fine-grained, porous structure with an uneven particle distribution. The average grain size is 0.5÷1.5 μm, and they are agglomerated into larger conglomerates. The grains are predominantly rounded, have poorly defined grain boundaries, and a smooth surface without faceting, indicating incomplete completion of the crystallization and sintering processes. The microstructure contains micropores of 2÷3 μm in

size, distributed over the surface of the material. The presence of porosity and intergranular defects indicates limited crystallite growth under the given heat treatment conditions and is associated with insufficient temperature or duration of calcination, which prevents the formation of a dense polycrystalline matrix. This morphology can lead to a decrease in the density and electrical strength of the material, but simultaneously increases the number of interphase boundaries, which has a positive effect on the dielectric characteristics due to increased polarization in the grain boundary regions [41, 42]. In general, the type A microstructure reflects the early stage of $BiFeO_3$ sintering and is formed at relatively low temperatures, when diffusion processes are not yet sufficiently intense. However, the presence of pores negatively affects the density and electrical strength of the sample, which requires optimization of the synthesis temperature regime. Consequently, the type A $BiFeO_3$ microstructure is characterized by fine grain size, moderate porosity, and surface heterogeneity, indicating incomplete completion of the sintering and crystallization stages under the given heat treatment conditions [43].

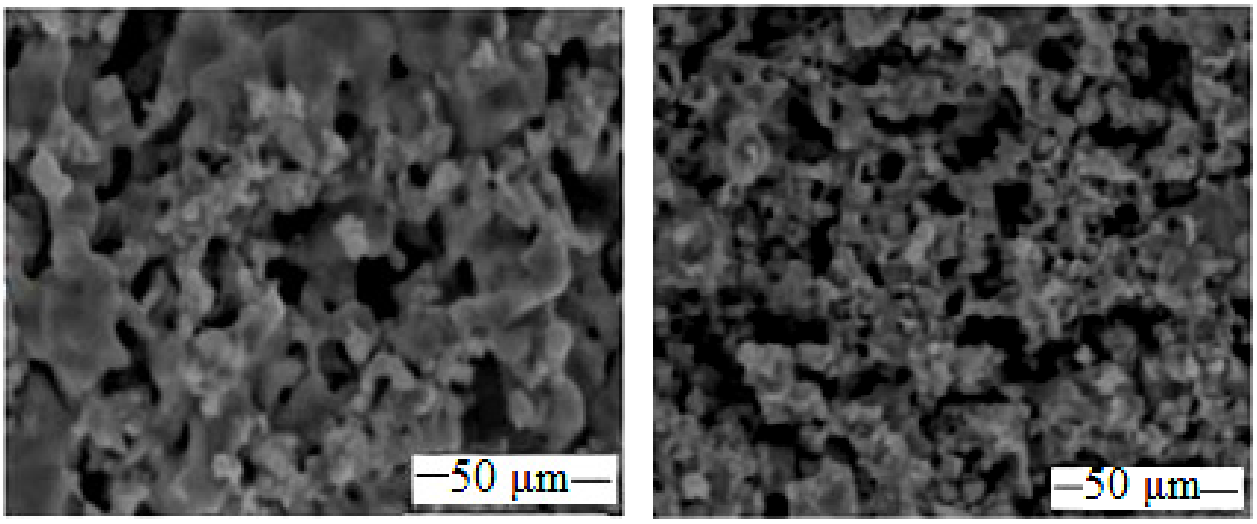

a b

Figure 3. SEM images of the $BiFeO_3$ microstructure surface:
a) type A; b) type B

The type B microstructure (Fig. 3b) has a denser and more uniform structure with clearly distinguishable grains. The average grain size increases to 1.5÷3.0 μm, indicating the occurrence of crystallite growth and coalescence processes. Pores are practically absent, the sample surface becomes smoother, and the grains form a compact matrix. This microstructure is formed at higher heat treatment temperatures, ensuring complete sintering and improved physical and mechanical properties [44]. Comparative analysis shows that an increase in the synthesis temperature promotes grain coarsening and decreases porosity, which is associated with the activation of diffusion processes in the solid phase. The evolution of the microstructure from type A to type B reflects the transition from a partially sintered state to a dense polycrystalline structure characteristic of the thermodynamically stable $BiFeO_3$ phase. Such changes have a direct impact on the functional properties of the material – an increase in density and grain size can contribute to an increase in electrical conductivity and a reduction in dielectric losses.

The values of apparent density (ρ_{app}), porosity (P), relative density (ρ_{rel}), structural looseness (ω), and the coefficient of linear thermal expansion (α) for two types of ceramic bismuth ferrite samples prepared from different starting components and synthesized by different methods are given in Table 2.

Table 2. Density and thermal parameters of ceramic bismuth ferrite samples

Samples	P_{app}, g/cm^3	P, %	P_{rel}, %	ω	α.10^6, K^{-1}
A-type	5.40	36	64.36	7.36	13.4
B-type	4.87	42	58.04	11.44	11.9

Type A samples exhibit higher apparent density (5.40 g/cm³) and relative density (64.36%) compared to type B samples (4.87 g/cm³ and 58.04%). Accordingly, the porosity of sample A is lower (36%) compared to B (42%), and the structural looseness is also lower and is 7.36 compared to 11.44. The difference in the structural looseness of the samples is due to the fact that the preliminary melting of oxides in a solar furnace promotes the formation of bismuth ferrite with a denser and more uniform crystalline structure, which is confirmed by the increased density and uniform microstructural structure of type A samples. The coefficient of linear thermal expansion α for samples A is higher (13.4×10^{-6} K^{-1}) than for samples B (11.9×10^{-6} K^{-1}). This is due to lower porosity and a denser crystalline structure, which ensures more pronounced thermal mobility of the lattice upon heating [45, 46]. It should be noted that the sintering of bismuth ferrite is somewhat improved when it is synthesized from pre-melted oxides. The processing of the starting components has a significant impact on the density characteristics and thermal stability of $BiFeO_3$ ceramic samples, which should be taken into account when developing materials with specified physical and mechanical properties [47-49].

Data on the phase composition of bismuth ferrite obtained from Fe_2O_3 and Bi_2O_3 oxides with different pre-treatments are given in Table 3.

Table 3. Results of bismuth ferrite synthesis depending on the pre-treatment of Fe_2O_3 and Bi_2O_3 components

Pretreatment of Fe_2O_3 and Bi_2O_3 components	Technological mode	Phase composition, %	
		$BiFeO_3$	$Bi_2Fe_4O_9$
not melted in a solar furnace	885 ^{0}C, 5 hours	88	12
melted in a solar furnace		97	3

The data show that the samples synthesized from molten oxides contain significantly less $Bi_2Fe_4O_9$ impurity phase (3%), whereas in the samples obtained from unmelted oxides, the content of the impurity phase reaches 12%. This difference may be due to the increased reactivity of the molten oxides, which accelerates the formation of the main $BiFeO_3$ phase and simultaneously promotes the appearance of the $Bi_2Fe_4O_9$ impurity phase at a lower temperature [50]. Preliminary melting of the oxides in a solar furnace ensures the formation of bismuth ferrite with a higher degree of purity and a smaller amount of secondary phases during synthesis at 885 °C for 5 hours. These results indicate the importance of choosing the form of the starting components for the synthesis of $BiFeO_3$ with high phase purity, which is important for optimizing the physical and chemical properties of the resulting material.

CONCLUSIONS

The conducted studies have shown that the thermal behavior of the Bi_2O_3-Fe_2O_3 system and the formation of bismuth ferrite depend significantly on the pretreatment of the starting oxides. It was found that the synthesis of $BiFeO_3$ from the starting materials begins at 790-850 °C, while its decomposition occurs at temperatures above ~920 °C. Preliminary melting of the oxides in a solar furnace leads to a shift in the thermal effects to higher temperatures and an increase in the thermodynamic stability of the resulting phase. X-ray diffraction analysis of samples calcined at 885 °C confirmed the formation of a perovskite-like structure with orthorhombic distortion and a high degree of crystallinity. The calculated lattice parameters and X-ray density correspond to the values for stable $BiFeO_3$, and the absence of reflections from secondary phases indicates the production of a phase-pure material. The average crystallite size, determined using the Scherrer formula, was 40±10 nm, which confirms the nanocrystalline nature of the formed structure.

Microstructural analysis revealed differences between samples obtained from molten and unmelted oxides. Type A material is characterized by a fine-grained, porous structure corresponding to the early stage of sintering, while type B samples exhibit a dense, homogeneous polycrystalline matrix with coarse grains. These differences are consistent with the density characteristics: type A samples have lower porosity and higher density. Phase analysis confirmed that the use of pre-melted oxides increases the content of the main $BiFeO_3$ phase to 97 % and reduces the proportion of the $Bi_2Fe_4O_9$ impurity phase. This is due to the increased reactivity of the oxides after solar melting and more complete solid-phase interaction.

Thus, solar pre-melting of Bi_2O_3 and Fe_2O_3 oxides is an effective technological approach that significantly increases the phase purity, crystallinity, and structural homogeneity of bismuth ferrite, as well as improves its physicochemical and functional properties. The obtained results confirm the potential of this method for creating high-quality $BiFeO_3$-based ceramic materials.

ORCID

Feruza A. Giyasova, https://orcid.org/0000-0003-0746-4986; **Murodjon A. Yuldoshev,** https://orcid.org/0000-0002-9722-9439
Farkhod A. Giyasov, https://orcid.org/0009-0003-9882-0655

REFERENCES

[1] Shuai Dong, Hongjun Xiang and Elbio Dagotto, "Magnetoelectricity in multiferroics: a theoretical perspective," National Science Review, **6,** 629-641 (2019). https://doi.org/10.1093/nsr/nwz023
[2] Sh.B. Utamuradova, Z.T. Azamatov, A.I. Popov, M.R. Bekchanova, M.A. Yuldoshev, and A.B. Bakhromov, East Eur. J. Phys. (3), 278 (2024). https://doi.org/10.26565/2312-4334-2024-3-27
[3] Yu. Gao, M.Yu. Gao, and Yu. Lu, "Two-dimensional multiferroics," Nanoscale, **13**, 19324-19340, (2021). https://doi.org/10.1039/d1nr06598j
[4] G. Catalan, and J.F. Scott, "Physics and Applications of Bismuth Ferrite," Advanced Materials, **21**(24), 2453-2556, (2009). https://doi.org/10.1002/adma.200802849
[5] B. Xu, D. Wang, J. Íñiguez, and L. Bellaiche, "Finite-Temperature Properties of Rare-Earth-Substituted $BiFeO_3$ Multiferroic Solid Solutions," Advanced Functional Materials, **25**(4), 497-650 (2015). https://doi.org/10.1002/adfm.201403811
[6] S. Zheng, J. Wang, J. Zhang, H. Ge, Z. Chen, and Y.F. Gao, "The structure and magnetic properties of pure single phase $BiFeO_3$ nanoparticles by microwave-assisted sol-gel method," Journal of Alloys and Compounds, **735**, 945-949, (2018). https://doi.org/10.1016/j.jallcom.2017.10.133
[7] S.F. Samadov, N.V.M. Trung, A.A. Sidorin, S.I. Ibragimova, S.H. Jabarov, M.A. Yuldoshev, O.S. Orlov, Y.I. Aliyev, Micro and Nanostructures 209 (2026) 208451, (2026). https://doi.org/10.1016/j.micrna.2025.208451

[8] A. Perejón, E. Gil-González, P.E. Sánchez-Jiménez, A.R. West, and L.A. Pérez-Maqueda, "Electrical properties of bismuth ferrites: $Bi_2Fe_4O_9$ and $Bi_{25}FeO_{39}$," Journal of the European Ceramic Society, **39**(2-3), 330-339 (2019). https://doi.org/10.1016/j.jeurceramsoc.2018.09.008
[9] A. Kirsch, G.B. Strapasson, N.L.M. Gogolin, M.C. Videbæk, S. Banerjee, H.N. Bordallo, and K.M. Ø. Jensen, "Control of Crystallization Pathways in the $BiFeO_3$-$Bi_2Fe_4O_9$ System," Chem. Mater. **37**, 338-348, (2025). https://doi.org/10.1021/acs.chemmater.4c02656
[10] A. Makridis, E. Myrovali, D. Sakellari, and M. Angelakeris, "Tuning the Structural and the Magnetic Properties of $BiFeO_3$ Magnetic Nanoparticles," Physica status solidi (b), **257**(6), (2020). https://doi.org/10.1002/pssb.202000005
[11] A.G. Monteduro, S.R.Ch. Leo, Sh. Karmakar, F. Sirsi, A. Leo, V. Tasco, M. Esposito, *et al*., "Dielectric and Ferroelectric Response of Multiphase Bi-Fe-O Ceramics," Physica status solidi (a), Vol. 216, Issue **3,** (2019). https://doi.org/10.1002/pssa.201800584
[12] G. Clarke, A. Rogov, S. McCarthy, L. Bonacina, Yu. Gun'ko, Ch. Galez, R.Le. Dantec, *et al*., "Preparation from a revisited wet chemical route of phase-pure, monocrystalline and SHG-efficient $BiFeO_3$ nanoparticles for harmonic bio-imaging," Scientific Reports, **8**, 10473 (2018). https://doi.org/10.1038/s41598-018-28557-w
[13] S.M. Selbach, M.A. Einarsrud, and T. Grande, "On the Thermodynamic Stability of $BiFeO_3$," Chemistry of Materials, **21**(1), 169-173 (2009). https://doi.org/10.1021/cm802607p
[14] F. Schröder, N. Bagdassarov, F. Ritter, and L. Bayarjargal, "Temperature dependence of Bi_2O_3 structural parameters close to the α-δ phase transition," Phase Transitions, **83**(5), 311-325 (2010). https://doi.org/10.1080/01411591003795290
[15] C. Wesley, L. Bellcase, J.S. Forrester, E.C. Dickey, I.M. Reaney, and J.L. Jones, "Solid state synthesis of $BiFeO_3$ occurs through the intermediate $Bi_{25}FeO_{39}$ compound," Journal of the American Ceramic Society, (2023). https://doi.org/10.1111/jace.19702
[16] R. Palai, R.S. Katiyar, H. Schmid, P. Tissot, S.J. Clark, J. Robertson, S.A. T. Redfern, *et al*., "β phase and γ-β metal-insulator transition in multiferroic $BiFeO_3$," Phys. Rev. B, **77**, 014110 (2008). https://doi.org/10.1103/PhysRevB.77.014110
[17] W. Song, D. Zhang, Z. Sun, B. Han, L.-J. He, and X. Wang, "Preparation and characterization of multiferroic $BiFeO_3$," in: *IEEE 10th International Conference on the Properties and Applications of Dielectric Materials*, (2012). https://doi.org/10.1109/ICPADM.2012.6318899
[18] A. Varma, A.S. Mukasyan, A.S. Rogachev, and K.V. Manukyan, "Solution Combustion Synthesis of Nanoscale Materials," Chem. Rev. **116**, 14493-14586, (2016). https://doi.org/10.1021/acs.chemrev.6b00279
[19] F. Siddique, S. Gonzalez-Cortes, A. Mirzaei, T. Xiao, M.A. Rafiq, and X. Zhang, "Solution combustion synthesis: the relevant metrics for producing advanced and nanostructured photocatalysts," Nanoscale, **14**, 11806-11868 (2022). https://doi.org/10.1039/D2NR02714C
[20] N. Asefi, M. Hasheminiasari, and S.M. Masoudpanah, "Photocatalytic properties of $BiFeO_3$ powders synthesized by the mixture of CTAB and Glycine, Scientific Reports, **13**, 12338 (2023). https://doi.org/10.1038/s41598-023-39622-4
[21] M.M. Suleimanova, M.U. Nosirova, H.T. Yusupov, and Kh.Yu. Rakhimov, "Wave-packet dynamics in monolayer graphene with periodic scattering potentials," Physica B: Condensed Matter, **714**, 417484 (2025). https://doi.org/10.1016/j.physb.2025.417484
[22] J. Rodriguez, I. Cañadas, and E. Zarza, "New PSA high concentration solar furnace SF40," AIP Conf. Proc. **1734**, 070028 (2016). https://doi.org/10.1063/1.4949175
[23] L.G. Rosa, "Solar Heat for Materials Processing: A Review on Recent Achievements and a Prospect on Future Trends," Chem. Engineering, **3**, 83 (2019). https://doi.org/10.3390/chemengineering3040083
[24] Y. Zhuang, X. Pan, X. Liu, and K. Chen, "Effect of Cooling Rate on the Crystalline Morphology of Bi_2O_3-Fe_2O_3 Pseudo-Binary System," Physica status solidi (a), **220**(9), (2023). https://doi.org/10.1002/pssa.202200838
[25] G. Levêque, R. Bader, W. Lipinski, and S. Haussener, "High-flux optical systems for solar thermochemistry," Solar Energy, **156**, 133-148 (2017). https://doi.org/10.1016/j.solener.2017.07.046
[26] M.S. Paizullakhanov, R.Yu. Akbarov, Zh.Z. Shermatov, O.T. Razhamatov, F. Ernazarov, M. Sulaimanov, N. Karshieva, *et al.*, "Small solar furnace for processing and melting of materials," in: *Collection of materials of the international scientific and technical conference "Actual problems of the energy complex: production, transmission and ecology*," (Karshi, 2024), pp. 533-538.
[27] V. Nicola, Y. Scarlett, and I.C. Madsen, "Quantification of phases with partial or no known crystal structures," Powder Diffraction, **21**(4), 278–284 (2016). https://doi.org/10.1154/1.2362855
[28] H.T. Costi, R. Dall'Agnol, M. Pichavant, and O.T. Ramo, "The peralkaline tin-mineralized madeira cryolite albite-rich granite of Pitinga, Amazonian craton, Brazil: petrography, mineralogy and crystallization processes," The Canadian Mineralogist, (2009). https://doi.org/10.3749/canmin.47.6.1301
[29] M.S. Paizullakhanov, and I.G. Atabaev, "BiFeO Synthesized on the Solar Furnace," Materials Research Letters, **1**(2), 1-4 (2017).
[30] M.S. Bernardo, "Synthesis microstructure and properties of $BiFeO_3$-based multiferroic materials: A review," Boletin de la Sociedad Espanola de Ceramica y Vidrio, **53**(1), 1-14, (2014). https://doi.org/10.3989/cyv.12014
[31] R. Haumont, I.A. Kornev, S. Lisenkov, L. Bellaiche, J. Kreisel, and B. Dkhil, "Phase stability and structural temperature dependence in powdered multiferroic $BiFeO_3$," Phys. Rev. B, **78**, 134108 (2008). https://doi.org/10.1103/PhysRevB.78.134108
[32] M.S. Paizullakhanov, A.A. Xolmatov, and M.M. Sobirov, "Magnetic materials synthesized in the sun furnace," International Journal of Advanced Research in Science, Engineering and Technology, **7**(4), 13499-13505 (2020).
[33] Kh. Bakhronov, O. Ergashev, G'. Ochilov, N. Esonkulova, A. Ganiev, N. Akhmedova, and O. Ochilova, "Study of isotherm, thermodynamic characteristics and sorption mechanism of toluene adsorption on zeolite CsZSM-5 by adsorption-calorimetric method. Edelweiss Applied Science and Technology, **8**(6), 6959-6966 (2024). https://doi.org/10.55214/25768484.v8i6.3508
[34] C.M. Suarez, S. Hernández, and N. Russo, "$BiVO_4$ as photocatalyst for solar fuels production through water splitting: A short review," Applied Catalysis A General, **504**, (2014). https://doi.org/10.1016/j.apcata.2014.11.044
[35] J. Matrasulov, J.R. Yusupov, and A.A. Saidov, "Fast forward evolution in heat equation: Tunable heat transport in adiabatic regime," Nanosystems: Phys. Chem. Math. **14**(4), 421-427 (2023). https://doi.org/10.17586/2220-8054-2023-14-4-421-427
[36] O.R. Furtado, "Metal oxides and the thermochemical storage of solar energy," in: Chimica Oggi - Chemistry Today, **37**(2), 6-18 (2019). http://hdl.handle.net/10400.9/3187

[37] H. Liu, and X. Yang, "Structural, dielectric, and magnetic properties of $BiFeO_3$ -$SrTiO_3$ solid solution ceramics," Ferroelectrics, **500**(1), 310-317 (2016). https://doi.org/10.1080/00150193.2016.1230445
[38] M.A. Rusho, T.A. Ahmed, L.H. Saleh, S.W. Ghori, E. Muniyandy, S. Usanov, M. Latipova, *et al.*, "Design and synthesis of decorated palladium nanoparticles on chitosan-tannic acid modified magnetic nanoparticles and evaluation of its catalytic application in the Heck coupling reactions," Journal of Organometallic Chemistry, **1039**, 123773 (2025). https://doi.org/10.1016/j.jorganchem.2025.123773
[39] N. Lomanova, M.V. Tomkovich, V.V. Sokolov, and V.V. Gusarov, "Special features of formation of nanocrystalline $BiFeO_3$ via the glycine-nitrate combustion method," Russian Journal of General Chemistry, **86**(10), 2256-2262 (2016). https://doi.org/10.1134/S1070363216100030
[40] B. Wang, and D.A. Hall, "Structural evolution in $BiFeO_3$-$BaTiO_3$ ceramics via quenching strategy," Journal of Alloys and Compounds, **1044**, 184439 (2025). https://doi.org/10.1016/j.jallcom.2025.184439
[41] Z. Zeng, Q. Zhang, H. Wu, and M. Lan, "Influence of calcination temperature on structure and multiferroic properties of barium ferrite ceramics," Processing and Application of Ceramics, **16**(2), 106-114 (2022). https://doi.org/10.2298/PAC2202106Z
[42] Sh.B. Utamuradova, F.A. Giyasova, K.N. Bakhronov, M.A. Yuldoshev, M.R. Bekchanova, and B. Ismatov, "Current Transfer Mechanism in A Thin-Based Heterosystem Based on A^2B^6 Compounds," East Eur. J. Phys. (3), 325-335 (2025). https://doi.org/10.26565/2312-4334-2025-3-31
[43] Z. Cen, Y. Huabin, C. Zhou, and Q. Zhou, "Effect of sintering temperature on microstructure and piezoelectric properties of Pb-free $BiFeO_3$-$BaTiO_3$ ceramics in the composition range of large $BiFeO_3$ concentrations," Journal of Electroceramics, **31**(1-2), (2013). https://doi.org/10.1007/s10832-013-9803-2
[44] D. Szalbot, J.A. Bartkowska, K.Feliksik, and M. Bara, "Correlation Between Structure, Microstructure and Dielectric Properties of $Bi_7Fe_3Ti_3O_21$ Ceramics Obtained in Different Conditions," Archives of Metallurgy and Materials, **65**(2), 879 (2020). https://doi.org/10.24425/amm.2020.132834
[45] E. Gil-Gonzalez, A. Perejon, P.E. Sánchez-Jiménez, and M.J. Sayagues, "Phase-pure $BiFeO_3$ produced by reaction flash-sintering of Bi_2O_3 and Fe_2O_3," Journal of Materials Chemistry A, **6**(13), (2017). https://doi.org/10.1039/C7TA09239C
[46] F.A. Giyasova, and M.A. Yuldoshev, "Investigation of temporal characteristics of photosensitive heterostructures based on gallium arsenide and silicon," Chalcogenide Letters, 22(2), 123–129 (2025). https://doi.org/10.15251/CL.2025.222.123
[47] F.A. Giyasova, Kh.N. Bakhronov, M.A. Yuldoshev, I.B. Sapaev, R.G. Ikramov, F.A. Giyasov, M.R. Bekchanova, M.M. Qaxxarov, H.O Abdullayev, East Eur. J. Phys. 4, 461 (2025). https://doi.org/10.26565/2312-4334-2025-4-47
[48] F.A. Giyasova, A.Z. Rakhmatov, Kh.N. Bakhronov, M.A. Yuldoshev, F.A. Giyasov, A.N. Olimov, N.A. Sattarov, East Eur. J. Phys. 4, 397 (2025). https://doi.org/10.26565/2312-4334-2025-4-38
[49] N.Yu. Sharibaev, A.Q. Ergashov, S.B. Fazliddinov, R.G. Ikramov, M.A. Yuldoshev, A.A. Abdulxayev, Journal of Ovonic Research. Vol.21, No.6, (2025). https://doi.org/10.15251/JOR.2025.216.859
[50] C. Wesley, L. Bellcase, J.S. Forrester, E.C. Dickey, I.M. Reaney, and J.L. Jones, "Solid state synthesis of $BiFeO_3$ occurs through the intermediate $Bi_{25}FeO_{39}$ compound," Journal of the American Ceramic Society, **107**(6). 3716-3723 (2024). https://doi.org/10.1111/jace.19702

ОСОБЛИВОСТІ ТЕПЛОВОЇ ПОВЕДІНКИ ТА ФАЗОУТВОРЕННЯ $BiFeO_3$ З ВИКОРИСТАННЯМ ПРЕКУРСОРІВ АКТИВОВАНИХ СОНЯЧНИМ ПЛАВІННЯМ

М.С. Пайзуллаханов[1,2] Ф.А. Гіясова[3], М.А. Юлдошев[4], Ch.X. Тошпулатов[5], Р.У. Ерназаров[5], Ф.А. Гіясов[3], А. Урішев[6], А.Д. Палуанова[7]

[1]Інститут матеріалознавства Академії наук Республіки Узбекистан. Ташкент, Узбекистан
[2]Ферганський державний технічний університет, Узбекистан
[3]Міжнародний університет Кімьо в Ташкенті, Узбекистан
[4]Міжнародний університет Туран, Наманган, Узбекистан
[5]Ташкентський філіал Самаркандського державного університету ветеринарної медицини, тваринництва та біотехнології, Узбекистан
[6]Ташкентський інститут інженерів іригації та механізації сільського господарства, Національний дослідницький університет, Узбекистан
[7]Нукусський державний педагогічний інститут, Узбекистан

Досліджено вплив попередньої обробки оксидів Bi_2O_3 та Fe_2O_3 на синтез та структурні характеристики фериту вісмуту $BiFeO_3$. Було виявлено, що утворення $BiFeO_3$ починається при 790÷850 °C, а розкладання відбувається вище ~920 °C. Попереднє плавлення оксидів у сонячній печі зміщує теплові ефекти в бік вищих температур та підвищує термодинамічну стабільність фази. Рентгенофазовий аналіз виявив утворення перовскітоподібної структури з орторомбічним спотворенням, високою кристалічністю та розміром кристалітів 40±10 нм. Фазовий аналіз підтвердив збільшення вмісту основної фази до 97 % та зменшення домішкової фази $Bi_2Fe_4O_9$. Отримані результати підтверджують ефективність попереднього сонячного плавлення оксидів для синтезу високоякісних керамічних матеріалів на основі $BiFeO_3$.

Ключові слова: *сонячна піч; синтез; ферит вісмуту; фаза; дифузія; мікроструктура; аналіз; температура; тепловий ефект*